General Disclaimer

One or more of the Following Statements may affect this Document

- This document has been reproduced from the best copy furnished by the organizational source. It is being released in the interest of making available as much information as possible.

- This document may contain data, which exceeds the sheet parameters. It was furnished in this condition by the organizational source and is the best copy available.

- This document may contain tone-on-tone or color graphs, charts and/or pictures, which have been reproduced in black and white.

- This document is paginated as submitted by the original source.

- Portions of this document are not fully legible due to the historical nature of some of the material. However, it is the best reproduction available from the original submission.

NASA Technical Memorandum 74085

THE USE OF LIDAR FOR STRATOSPHERIC MEASUREMENTS

M. P. McCormick

September 1977

National Aeronautics and Space Administration

Langley Research Center
Hampton, Virginia 23665

THE USE OF LIDAR FOR STRATOSPHERIC MEASUREMENTS*

M. Patrick McCormick

Langley Research Center

ABSTRACT

This paper reviews stratospheric measurements possible with ground-based, airborne, and satellite-borne lidar systems. The instruments, basic equations, and formats normally used for various scattering and absorption phenomena measurements are presented including a discussion of elastic, resonance, Raman, and fluorescence scattering techniques.

INTRODUCTION

The heart of a lidar system is the laser which was first conceived by Professors Schalow and Townes in December 1958 at Columbia. It was not until May 1960 that Dr. Theodore Maiman at Hughes Research Laboratory first reduced the laser principle to practice. Actually the term lidar, an acronymn for light detection and ranging, came before the advent of the laser. Middleton and Spilhaus in their 1953 book on "Meteorological Instruments" first suggested the term "lidar" for light detection and ranging when discussing ceilometry. The honor of the first paper in which data were described using a lidar goes to Fiocco and Smullin for their September 1963 paper "Detection of Scattering Layers in the Upper Atmosphere (60-140 km) by Optical Radar." This was followed by a paper by Fiocco and Grams (May 1964) entitled "Observations of the Aerosol Layer at 20 km by Optical Radar." During this early period, papers were being presented and published in which the potential uses of lasers and lidar in meteorology were being expounded. As an example, Goyer and Watson at NCAR published a paper on "The Laser and Its Application to Meteorology" in September 1963. Myron Ligda gave a paper in September 1964 at the World Conference on Radio Meteorology in which he pointed out that others were also discussing the possible uses of lasers in meteorology. These included Dick Schotland, Dave Atlas, P. S. Carter, and R. B. Battelle. Also described in this presentation was the first Stanford Research Institute (SRI) lidar (Mark I) which was built in January 1963. Initial atmospheric returns were obtained in July 1963, and they were the first to apply the lidar technique to meteorology in the lower troposphere.

Most lidar measurements have utilized elastic scattering techniques but more recently have also included inelastic scattering and absorption studies. Presently, many groups are working with lidar in an attempt to characterize the atmosphere. For an idea of the scope of this work, see the various

*Invited Paper: 8th International Laser Radar Conference, Drexel University, Philadelphia, Pa., June 6-9, 1977.

Conference Abstracts of the Conferences on Laser Radar Studies of the Atmosphere. A comprehensive review of lidar measurements of the atmosphere can be found in E. D. Hinkley (1976).

In general, laser radars operate in the following manner. A Q-switched laser emits a pulse of nearly monochromatic light approximately 30 nsec in duration into the atmosphere. Molecules and suspended particulate matter (aerosols) scatter and/or absorb this radiation as the pulse propagates through the atmosphere. A small portion of this light is scattered directly back toward the laser. A receiver composed of mirrors and/or lenses collects this backscattered radiation and directs it onto a photodetector whose output is measured as a function of elapsed time after laser emission or, therefore, range. The backscattered energy incident on the photodetector is examined spectrally at or near the laser output wavelength with color filters, interference filters, or spectrometers. This enhances the signal-to-noise ratio by reducing unwanted background radiation and determines whether elastic or inelastic techniques are utilized.

An example of a system for stratospheric measurements is the Langley Research Center's 48" laser radar system. It consists of two temperature-controlled lasers (ruby and neodymium-doped glass) mounted alongside an f/10 Cassegrainian-configured telescope consisting of a 48-inch diameter f/2 all metal primary and a 10-inch diameter secondary. The output from the detector package is recorded by a high-speed data acquisition system. Analog signals are amplified and bandwidth limited, digitized at a 5- or 10-megahertz rate with 8-bit accuracy, and recorded on magnetic tape. Pulse count data is amplified, discriminated, counted at a 200 megahertz rate, and also stored on magnetic tape. Altitude resolution is obtained by using the variable 1-, 5-, or 10-microsecond bin widths that are available. A 16K word storage computer is used to control the data acquisition system and provide data massage. An X-band microwave radar, boresighted with the laser system axis, is used to ensure safe operation in the atmosphere. A rotating shutter in front of the laser reduces laser fluorescence after Q-switching. The entire system is mobile and can scan in elevation and azimuth at a slew rate of 1° per second.

LIDAR THEORY

After crossover of the emitted laser pulse and receiver field of view, the voltage $V(\lambda,R)$ at the photodetector output for a laser radar system is given by

$$V(\lambda,R) = \frac{\gamma(\lambda)E(\lambda)q_t(\lambda,\Delta R)q_s(\lambda',\Delta R)f(\lambda,R)}{R^2} \qquad (1)$$

with

$$\gamma(\lambda) = \frac{cA}{2} T(\lambda)S(\lambda)L$$

where $f(\lambda,R)$ is the backscattering function at wavelength λ and range R, and $q_t(\lambda,\Delta R)$ and $q_s(\lambda',\Delta R)$ are the transmissivities from the laser radar to the scattering volume and from the scattering volume to the laser radar, respectively. The symbol λ' refers to a wavelength that may not be λ. L is the photodetector load resistor, $T(\lambda)$ is the system optical efficiency, $S(\lambda)$ is the photodetector spectral sensitivity, A is the area of the receiver, c is the speed of light, and $E(\lambda)$ is the laser output energy per pulse.

For elastic scattering, the emitted and return wavelengths are identical. Equation (1) reduces to

$$V(\lambda,R) = \frac{\gamma(\lambda)E(\lambda)q^2(\lambda,\Delta R)f(\lambda,R)}{R^2} \tag{2}$$

where $f(\lambda,R) = f_M(\lambda,R) + f_A(\lambda,R)$. The subscripts M and A refer to molecular and aerosol, respectively. The Raman scattered return is shifted in wavelength from the laser output and equation (1) becomes

$$V(\lambda',R) = \frac{\gamma(\lambda')E(\lambda)q_t(\lambda,\Delta R)q_s(\lambda',\Delta R)f_r(\lambda',R)}{R^2} \tag{3}$$

where $f_r(\lambda',R)$ is the Raman scattering function at R and is independent of aerosol scattering. The shift in wave numbers is characteristic of the particular molecular species in the scattering volume. Raman scattering can occur for any incident wavelength but its scattering function is approximately three orders of magnitude less than molecular scattering functions.

For the case of fluorescence scattering, λ' may or may not be λ with the scattering function being that of fluorescence scattering. It can only occur, however, when λ corresponds to an absorption line or band in the atmosphere and, like Raman scattering, the return radiation at λ' is characteristic of the fluorescing molecules. Although the cross sections for fluorescence are very large compared to Raman scattering, there are inherent problems that must be overcome in order to utilize this technique. It now appears that the differential absorption laser radar technique (DIAL) might offer the best hope for measuring pollutants with laser radar.

An atmospheric scattering model for the elastic backscattering function at two laser wavelengths is shown in figure 1. The details of its derivation are

given by McCormick (1971). The molecular contribution is calculated by using the familiar Rayleigh scattering equation and the U. S. Standard Atmosphere (1962). The aerosol contribution is calculated assuming: Mie theory, a Junge r^{-4} size distribution from 0.125 μm to 10 μm; a 1.5 refractive index; and Rosen's (1966) particle sampling data from 5 to 26 km with a sea level value of 450 particles/cm^3 and an exponential interpolation between sea level and 5 km. This model includes this interpolation since the aerosol number density in the first 5 km is highly variable. From equation (2) it is evident that the laser radar signal is dependent upon a combination of both aerosol and molecular scattering through the transmissivity,

$$q^2(\lambda,R) = \exp(-2\tau) = \exp\left[-2\int_0^R \beta(\lambda,R')dR'\right] \tag{4}$$

where τ is the optical depth and β is the extinction coefficient, and through the aerosol and molecular scattering functions. The molecular scattering contribution is very easy to calculate (Rayleigh scattering) but the aerosol contribution cannot be easily (and not uniquely) determined. Usually spherical aerosols of an assumed size distribution and refractive index are used with Mie scattering theory to calculate the aerosol contribution.

A combination of Raman and elastic scattering, however, might also be used to determine aerosol scattering functions. The ratio of the Raman return at two altitudes Z_1 and Z_2 can be written from equation (3) as

$$\frac{Z_1^2 V(\lambda',Z_1)}{Z_2^2 V(\lambda',Z_2)} = \frac{q(\lambda,0-Z_1)q(\lambda',Z_1-0)\sigma_r N(Z_1)}{q(\lambda,0-Z_2)q(\lambda',Z_2-0)\sigma_r N(Z_2)} \tag{5}$$

where σ_r is the Raman cross section for the particular gas molecule of number density N and $q(\lambda,0-Z_1)$ is the transmissivity at λ from the laser radar to altitude Z_1.

Assuming $q(\lambda,\Delta Z) = q(\lambda',\Delta Z)$, equation (5) becomes

$$\frac{Z_1^2 V(\lambda',Z_1)}{Z_2^2 V(\lambda',Z_2)} = \frac{1}{q^2(\lambda',Z_1-Z_2)} \quad \frac{N(Z_1)}{N(Z_2)} \tag{6}$$

This assumption is good when there is no differential absorption or large extinction between λ and λ'. Taking the natural logarithm of both sides of equation (6) gives

$$\int_{Z_1}^{Z_2} 2\,\beta(\lambda', Z)dZ = \frac{-1}{2} \ln \frac{Z_2^2 V(\lambda', Z_2)N(Z_1)}{Z_1^2 V(\lambda', Z_1)N(Z_2)} \tag{7}$$

Assuming β constant over Z_1 to Z_2 gives

$$\beta(\lambda', \bar{Z}) = \frac{-1}{2(Z_2 - Z_1)} \ln \frac{Z_2^2 V(\lambda', Z_2)N(Z_1)}{Z_1^2 V(\lambda', Z_1)N(Z_2)} \tag{8}$$

The number densities for air at the two altitudes can be obtained from rawinsonde temperature and pressure data. Then β can be used in Koschmieder's equation to find meteorological range. Or this value of the total extinction coefficient can be used with equation (4) to determine the two-way transmissivity and the value of q^2 obtained in this manner can be used in equation (2) for elastic scattering. The Raman nitrogen data ratioed at three altitudes combined with simultaneous elastic scattering data ratioed at the same three altitudes will yield three equations and three unknowns from which the aerosol scattering function at the three altitudes can be uniquely determined. Other techniques for using laser radar data are discussed in a paper by McCormick and Fuller (1973).

Normally, stratospheric aerosol lidar data is presented in terms of the backscattering ratio

$$R'(\lambda, Z) = Z^2 V(\lambda, Z)/q^2 f_M(\lambda, Z) \tag{9}$$

or using equation (2)

$$R'(\lambda, Z) = \gamma E(\lambda) \frac{f_A(\lambda, Z) + f_M(\lambda, Z)}{f_M(\lambda, Z)} \tag{10}$$

The lidar total backscatter ratio $R(\lambda, Z)$ can be determined by multiplying $R'(\lambda, Z)$ with a conversion constant K such that

$$\begin{aligned} R(\lambda, Z) &= K\, R'(\lambda, Z) \\ &= 1 + f_A(\lambda, Z)/f_M(\lambda, Z) \end{aligned} \tag{11}$$

Since the lidar system calibration factor is unknown, the constant K has to be determined by normalizing the ratio $R'(\lambda,Z)$ in an altitude region where backscattering is assumed to be only from molecules. This normalization can be performed by searching for the minimum value of $R'(\lambda,Z)$ in the altitude range from the tropopause to 32 km for each profile. The exact altitude where aerosol backscattering is assumed negligible depends on varied factors such as the approximate aerosol content of the stratosphere (fresh volcanic, background volcanic, etc.), seasonal variations in the aerosol profile, lidar wavelengths, etc. The minimum value of $R(\lambda,Z)$ found is assumed to be due to molecular backscattering alone and used to normalize the backscattered profile. As described above the two-way atmospheric transmittance must also be determined either by assumed theoretical models or by a combination of Raman and elastic lidar backscattering. The sensitivity of $q^2(\lambda,Z)$ to various stratospheric aerosol loadings has been discussed in detail by Russell et al. (1976). If the proper normalization and transmittance are assumed, any ratio value greater than one indicates aerosol scattering.

STRATOSPHERIC MEASUREMENTS

Ground-Based

Lidars have been used extensively to study the lower stratosphere. Some of the earlier measurements are shown in figure 2 taken over Williamsburg, Virginia, March 18, 1967 (McCormick, 1967). At this period of time the stratospheric aerosol layer (Junge or sulfate layer), centered at approximately 18 km, was very evident in lidar backscatter signatures representing approximately twice the scattering expected from a molecular atmosphere.

Shown in figure 3 are examples of this scattering ratio plotted as a function of altitude for the period 1967-1974. After 1967, the stratospheric aerosol loading decreased and became quiescent until the eruption of the volcano de Fuego in Guatemala (14.5° N, 90.9° N). Large increases in stratospheric aerosol and their related optical effects were observed at different locations in the northern hemisphere (McCormick and Fuller, 1975; Fegley and Ellis, 1975; Meinel and Meinel, 1975; Volz, 1975). Additional data covering the period 1964 through 1974 are shown in figure 4 (Russell et al., 1975). They are compared with three other techniques used during this period. Despite the fact that the four observational methods observe different characteristics of the stratospheric aerosol, and the locations are different, the general trends all agree.

The data from another comparison study corroborating the lidar technique are shown in figure 5 (Northam et al., 1974). In this study the normalized lidar backscattering was used to infer the aerosol scattering function. The lidar data were compared with the Wyoming dustsonde derived aerosol concentration. The best fit was for aerosol scattering functions of 6 to 8 x 10^{-9} m^{-1} sr^{-1}. The agreement between the results from these two instruments is generally

quite good. Both measurements detected thin high altitude cirrus clouds, both describe the peak and approximate structure of the 20 km aerosol layer and both indicate a relatively aerosol free region above the troposphere.

Another comparison is shown in figure 6 (Russell et al., 1975). Data from the SRI lidar is compared with filter sample data taken aboard a WB-57 aircraft that flew over the lidar site. A calculation based upon the mass of collected particles and assumed particle model parameters for a modified gamma distribution of sulfuric acid particles yields the agreement in aerosol backscattering coefficient indicated.

A more recent comparison is shown in table 1 (Pepin et al., 1976). Here, lidar data are compared with dustsonde measurements and satellite limb extinction measurements. The results from these three different measurement techniques agree very well.

Some lidar data obtained after the de Fuego eruption are shown in figure 7 corresponding to four different months: November 1974, February 1975, July 1975, and July 1976. The dashed lines are rawinsonde-derived temperature profiles and the arrow indicates the location of the assumed tropopause. A summary of the gradual decay of the stratospheric aerosol after the de Fuego eruption is further shown in figure 8 (McCormick et al., 1977), where the aerosol backscattering coefficient profile has been integrated with altitude over different altitude intervals.

$$\int_{h_T}^{28} (R(\lambda,Z)-1) \cdot f_M(\lambda,Z)dZ \qquad (12)$$

where h_T is the height of the tropopause in km. This integral has been normalized to the value obtained from the lidar data of October 10, 1974. These data show an e-folding decay time of 11.6 months over the time period January 1975 to July 1976. From both winter to summer periods of 1975 and 1976 the data show an approximate 40 percent decrease in the aerosol integrated backscatter. The decrease of the total stratospheric aerosol integrated backscatter over a 1-year period from January 1975 to January 1976 is approximately 65 percent. These values are in relative agreement with estimates of the annual outflow of stratospheric air mass from the northern hemisphere (Reiter, 1975).

Another technique for measuring stratospheric aerosols is to use two wavelengths simultaneously, one sensitive primarily to aerosol scattering and the second to molecular scattering. Efforts have been made to analyze lidar backscattering data independently of rawinsonde data since the real time molecular scattering is needed in order to properly interpret the aerosol scattering ratio and the integrated aerosol column data, especially in times of low stratospheric loadings. Otherwise, rawinsonde data must be collected, used to construct the expected molecular scattering profile, and the lidar ratio formed as in equation (9). Figure 9 (Fuller et al., 1976) shows lidar

data at 0.6943 μm ratioed to 0.3472 μm lidar data as compared to lidar data at 0.6943 μm ratioed with the standard rawinsonde technique. Another approach to this problem is the use of Raman backscattering from nitrogen. Kent et al. (1971) in Jamaica measured Raman backscattering from nitrogen to a 40 km height. A comparison with rawinsonde-derived molecular density profiles showed good agreement.

Inaba (1976) has analytically shown the feasibility for measuring various gases in the atmosphere using Raman backscatter. His results indicate that Raman backscatter at night using a laser energy of 1 joule per pulse at 0.3472 μm and a receiving telescope of 0.5 m^2 area, can be used to probe oxygen and nitrogen to approximately 50 km height with 100 laser shots. His simulations use 1 km altitude intervals. H_2O, N_2O, NO, and O_3 were below the detection limits in the stratosphere, but he concluded that CO_2 should be measurable to approximately 15 km.

Other techniques such as near-resonance Raman scattering and resonance fluorescence are not feasible for stratospheric species measurements using present state-of-the-art instrumentation. Stratospheric ozone measurements, however, are on the threshold of present detection limits using differential wavelength and range absorption lidar measurement techniques. A balloon-borne or airborne lidar system for measuring various stratospheric species at short ranges, however, appears feasible.

Aircraft Measurements

Another stratospheric application of lidar was shown in a paper by Stanford (1975) on the temporal variation of lidar scattering from stratospheric condensation particles over polar regions. He proposed that these measurements could shed valuable light on the physics and meteorology involved in their formation by yielding information on the height, time, and horizontal variation of the water vapor mixing ratio.

The ability of an airborne lidar system for probing the stratosphere was clearly shown in a paper by Fernald and Schuster (1977). It showed that aerosols could vary systematically with the prevailing meteorology and that continuous airborne lidar measurements over large geographical areas could provide valuable means for studying stratospheric/tropospheric exchange processes.

Satellite Measurements

A number of lidar groups including SRI, Wisconsin, and NASA Langley Research Center are evaluating the feasibility of measuring atmospheric species from satellite altitudes (Wright et al., 1975; Shipley et al., 1975; and Remsberg and Northam, 1976). These studies show the possibility of measuring a number of atmospheric species from satellite altitudes. Because of the power and instrument size and weight requirements, these measurements will have to be

performed from space shuttle type platforms. The measurements that are feasible from such a system include: Spatial variations of cloud tops; subvisible cirrus cloud distribution, and in some instances cloud thickness; stratospheric aerosol distributions; tropospheric aerosol distributions when not obscured by thick clouds; atomic vapors such as sodium; several minor ions such as Mg^+; and possibly molecular constitutents such as O_2, N_2, H_2O, and O_3.

Figure 10 shows a stratospheric simulation using various aerosol models from Shettle and Fenn (1976): Fresh volcanic, aged volcanic, and background condition. The calculations are for a backscatter return at a spacecraft altitude of 260 km. The ordinate shows the number of photons per microsecond incident on a 1-meter-diameter mirror for a shuttle-borne Nd:YAG or Nd:glass laser emitting a single 1 joule pulse at 1.06 μm. It is possible with this signal level to detect the stratospheric aerosol to at least 30 km in nighttime viewing conditions. Figure 11 shows an example of the return from a fresh volcanic aerosol with and without a 1 km uniform cloud having an extinction coefficient of 2.9 km^{-1}. Cloud top determinations are possible to a resolution of the lidar range cell length in all viewing conditions (daytime and nighttime).

ACKNOWLEDGEMENT

The author would like to acknowledge the assistance of Dr. T. J. Swissler of Systems and Applied Sciences Corporation for critically reading this manuscript, offering many helpful suggestions, and performing some of the calculations presented.

REFERENCES

1. Fegley, R. W.; and H. T. Ellis: Lidar Observations of a Stratospheric Dust Cloud Layer in the Tropics, Geophys. Res. Let., 2, 139-141, 1975.

2. Fernald, F. G.; and Schuster, B. G.: Wintertime 1973 Airborne Lidar Measurements of Stratospheric Aerosols, J. Geophys. Res., 82, 433-437. 1977.

3. Fiocco, G.; and Smullin, L. D.: Detection of Scattering Layers in the Upper Atmosphere (60-140 km) by Optical Radar, Nature, 199, 1275-1276, 1963.

4. Fiocco, G.; and Grams, G.: Observations of the Aerosol Layer at 20 km by Optical Radar, J. Atm. Sci., 21, 323-324, 1964.

5. Fuller, W. H., Jr.; Swissler, T. J.; and McCormick, M. P.: Comparative Analysis of Red-Blue Lidar and Rawinsonde Data, in Atmospheric Aerosols: Their Optical Properties and Effects, NASA CP-2004, TUC2-1 to 4, 1976.

6. Goyer, G. G.; and Watson, Robert: The Laser and Its Application to Meteorology, Bull. Am. Meteor. Soc., 44, 564-570, 1963.

7. Hinkley, E. D. (Editor): Laser Monitoring of the Atmosphere, Springer-Verlag Berlin, Heidelberg, New York, 1976.

8. Inaba, H.: Detection of Atoms and Molecules by Raman Scattering and Resonance Fluorescence, in Hinkley, 153-237, 1976.

9. Kent, G. S.; Sandland, P.; and Wright, R. W. H.: A Second Generation Laser Radar, J. Appl. Meteor, 10, 443-452, 1971.

10. Ligda, M. G. H.: Meteorological Observations with Lidar, 1964 World Conference on Meteorology, Boulder, CO., American Meteorological Society, Boston, 482-489, 1964.

11. McCormick, M. P.: Laser Backscatter Measurements of the Lower Atmosphere, Ph.D. Thesis, College of William and Mary, Williamsburg, VA, 1967.

12. McCormick, M. P.: Simultaneous Multiple Wavelength Laser Radar Measurements of the Lower Atmosphere, Proc. of the Technical Programme, Electro-Optics '71 International Conf., Brighton, England, Industrial and Scientific Conference Management, Inc., Chicago, Ill., 495-512, 1971.

13. McCormick, M. P.; and Fuller, W. H., Jr.: Lidar Techniques for Pollution Studies, AIAA J., 11, 244-246, 1973.

14. McCormick, M. P.; Swissler, T. J.; Chu, W. P.; and Fuller, W. H., Jr.: Post-Volcanic Stratospheric Aerosol Decay as Measured by Lidar, submitted to J. Atm. Sci.

15. Meinel, A. B.; and Meinel, M. P.: Stratospheric Dust Aerosol Event of November 1974, Science, 188, 447-478, 1975.

16. Middleton, W. E. K.; and Spilhaus, A. F.: Meteorological Instruments, Univ. of Toronto Press, Toronto, ed. 3, 1953.

17. Northam, G. B.; Rosen, J. M.; Melfi, S. H.; Pepin, T. J.; McCormick, M. P.; Hormann, D. J.; and Fuller, W. H., Jr.: A Comparison of Dustsonde and Lidar Measurements of Stratospheric Aerosols, Appl. Opt., 13, 2416-2421, 1974.

18. Pepin, T. J.; and McCormick, M. P.: Stratospheric Aerosol Measurement, NASA TMX-58173, 9/1-9/8, 1976.

19. Remsberg, E. E.; and Northam, G. B.: Feasibility of Atmospheric Aerosol Measurements with Lidar from Space Shuttle, in Atmospheric Aerosols: Their Optical Properties and Effects, NASA CP-2004, TUC4-1 to 4, 1976.

20. Reiter, E. R.: Stratospheric-Tropospheric Exchange Processes, Rev. Geophys. Space Phys., 13, 459-474, 1975.

21. Rosen, J. M.: Correlation of Dust and Ozone in the Stratosphere, Nature, 209, 1342, 1966.

22. Russell, P. B.; Viezee, W.; Hake, R. D., Jr.; and Collis, R. T. H.: Lidar Observations of the Stratospheric Aerosol: Summary of Results and a Calibration-Error Assessment, Proceedings, Fourth Conf. on CIAP, DOT-TSC-OST-75-38, 497-508, 1975.

23. Russell, P. B.; Viezee, W.; Hake, R. H., Jr.; and Collis, R. T. H.: Lidar Observations of the Stratospheric Aerosol: California, October 1972 to March 1974, Quart. J. R. Met. Soc., 103, 675-695, 1976.

24. Shettle, E. S.; and Fenn, R. W.: Models of the Atmospheric Aerosols and Their Optical Properties, AGARD Optical Propagation in the Atmosphere, 27-31 Oct. 1975, CP-183, 2-1 to 2-16, 1976.

25. Shipley, S. T.; Joseph, J. [illegible]; Trauger, J. T.; Guetter, P. J.; Eloranta, E. W.; Lawler, J. E.; Wiscombe, W. J.; Odell, A. P.; Roesler, F. L.; and Weinman, J. A.: The Evaluation of a Shuttle Borne Lidar Experiment to Measure the Global Distribution of Aerosols and Their Effect on the Atmospheric Heat Budget, NTIS report number N76-16597, 1975.

26. Stanford, J. L.: Stratospheric Water Vapor Information from Laser-Radar Scattering Measurements, J. Atm. Sci., 32, 852-856, 1975.

27. Volz, F. E.: Volcanic Twilights from the Fuego Eruption, Science, 189, 48-50, 1975.

28. Wright, M. L.; Proctor, E. K.; Gasiorek, L. S.; and Liston, E. M.: A Preliminary Study of Air Pollution Measurements by Active Remote-Sensing Techniques, NASA CR-132724, 1975.

TABLE I AEROSOL OPTICAL MODEL

MODEL: LOG NORMAL
TOTAL PARTICLE NUMBER DENSITY $10/cm^3$
REFRACTIVE INDEX $n = 1.42$

	EXTINCTION AT 0.83 μm	RATIO OF* BACKSCATTER TO EXTINCTION	PARTICLE DENSITY**	
			DIAMETER > 0.3 μm	DIAMETER > 0.5 μm
EXPERIMENTALLY DETERMINED	1.1×10^{-3} km^{-1}	0.023	$3/cm^3$	$\sim 1/cm^3$
MODEL CALCULATION	1.21×10^{-3} km^{-1}	0.024	$3/cm^3$	$\sim 1/cm^3$

*RATIO OF LIDAR BACKSCATTER FUNCTION AT 0.7 μm TO EXTINCTION AT 0.83 μm.

**DUSTSONDE RESULTS

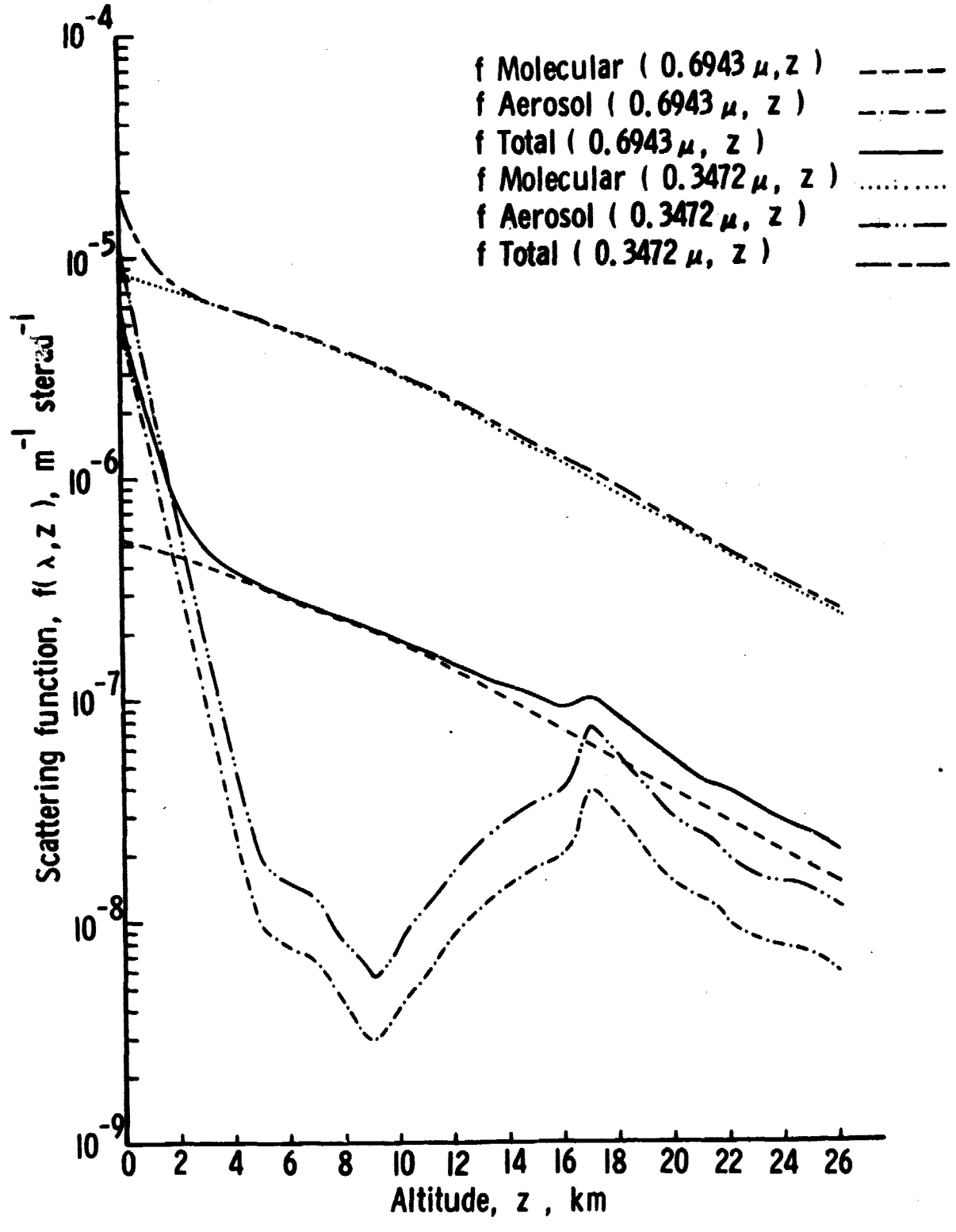

Figure 1.- Backscattering function model of the atmosphere for a wavelength of 0.6943 μm and 0.3472 μm. Molecular contribution, aerosol contribution, and their sum are shown.

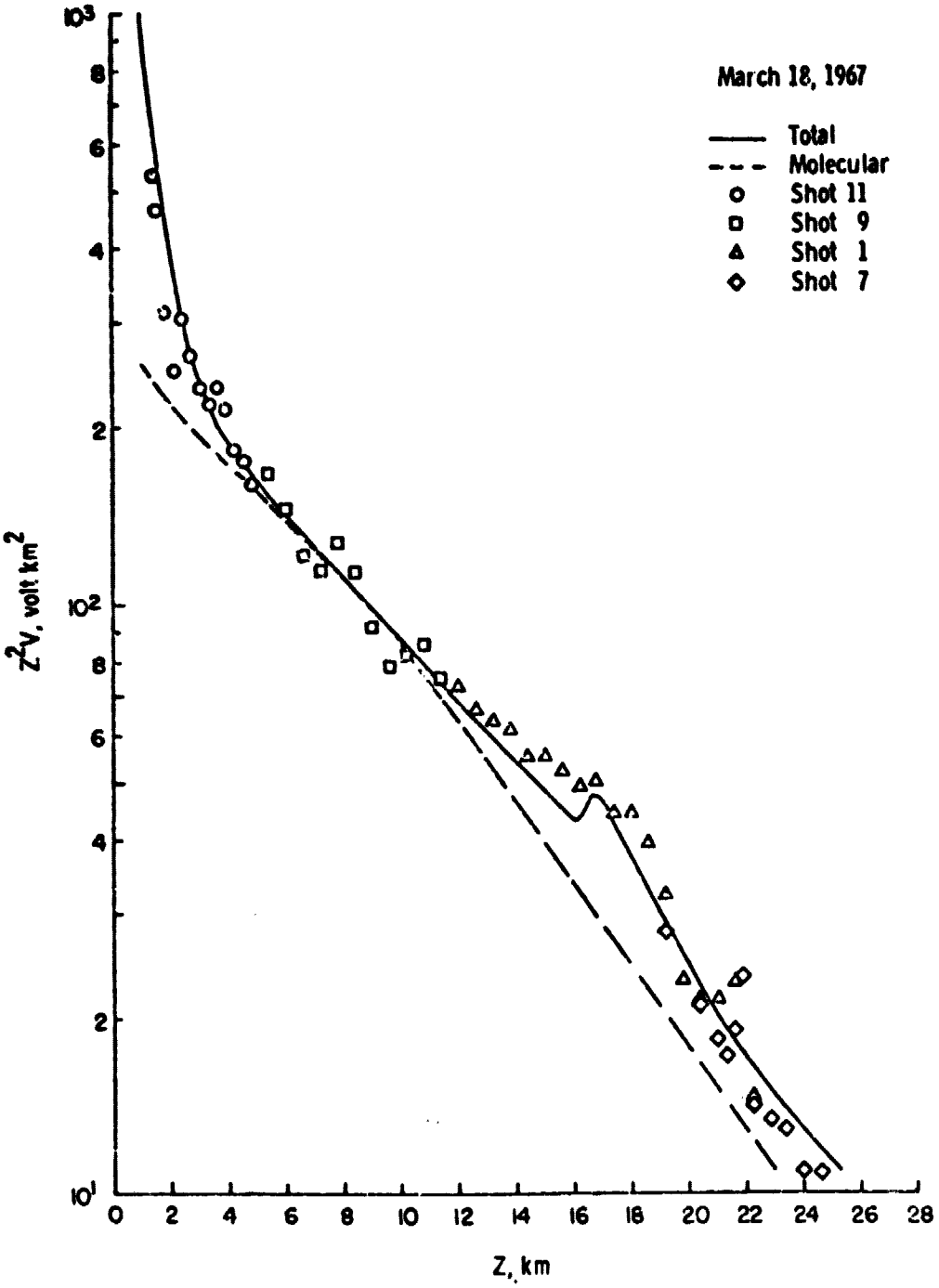

ure 2.- Range corrected backscatter return March 18, 1967, for a wavelength of 0.6943 μm.

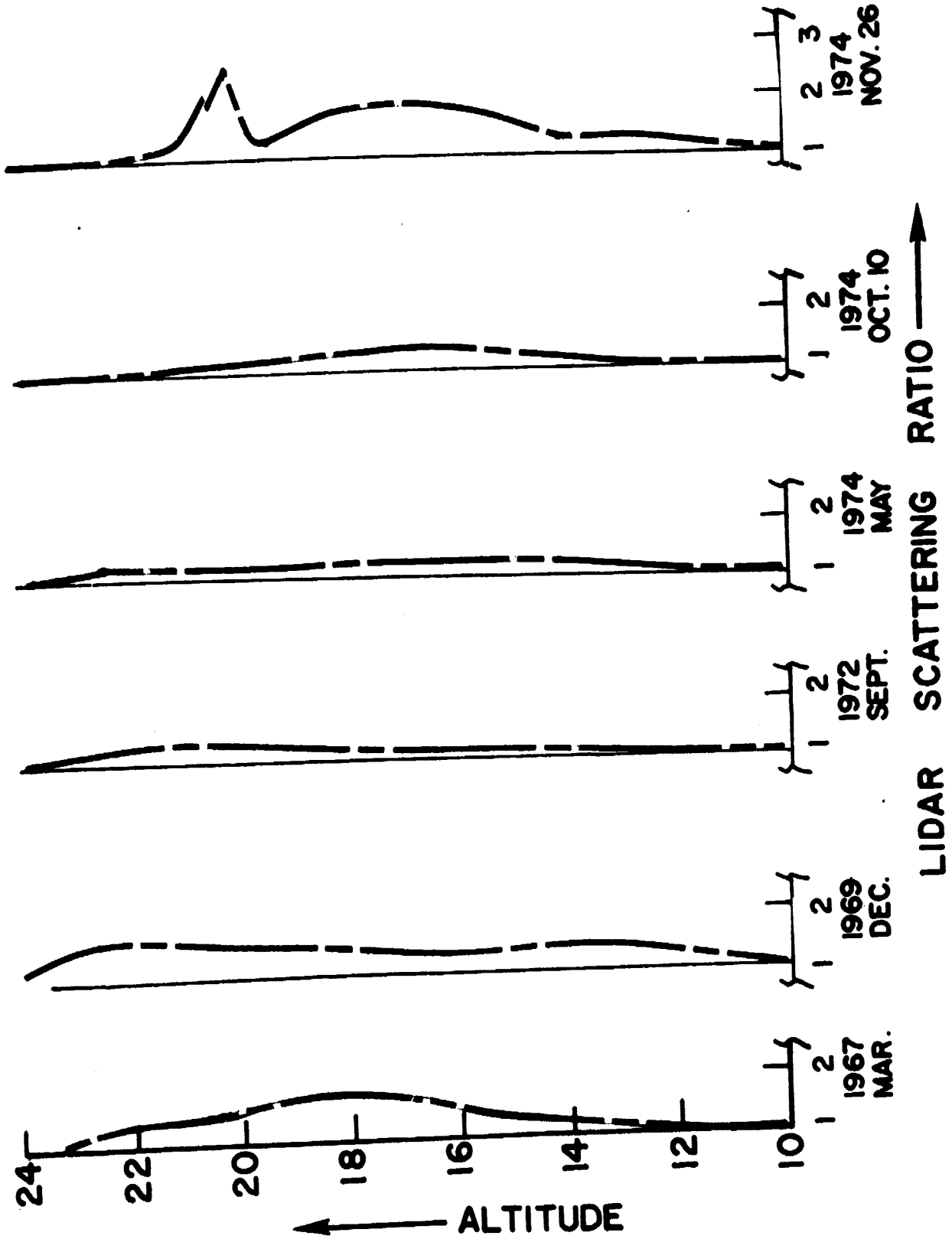

Figure 3.- Stratospheric lidar backscatter data 1967-1975.

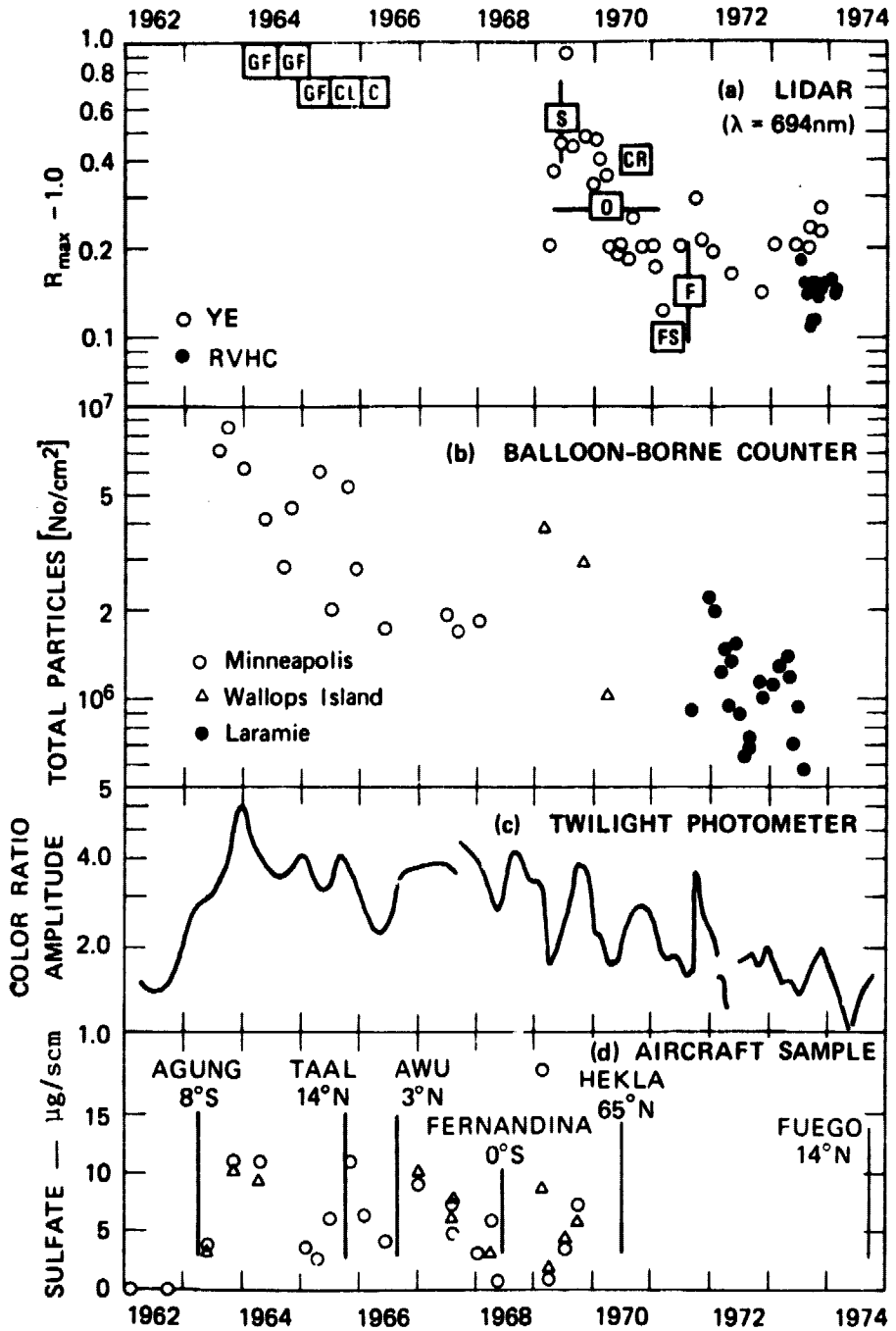

4.- Comparison of stratospheric aerosol measurements made by four independent techniques between 1962 and 1974. (a) Maximum value of peak aerosol backscatter ratio, (R-1.0) as observed by GF(Grams and Fiocco), CL(Collis and Ligda), C(Clemesha et al.), S(Schuster), CR(Clemesha and Rodriques), O(Ottway), FS(Fresh and Schuster), F(Fox et al.), YE(Young and Elford), RVHC(Russell, Veezee, Hake and Collis). (b) Number of particles above tropopause as measured by photoelectric particle counter (Hofmann et al.). (c) Color-ratio amplitude as measured by twilight photometer (Volz). (d) Mass of sulfate per standard cubic meter (scan), as collected on aircraft-borne filters (Castleman).

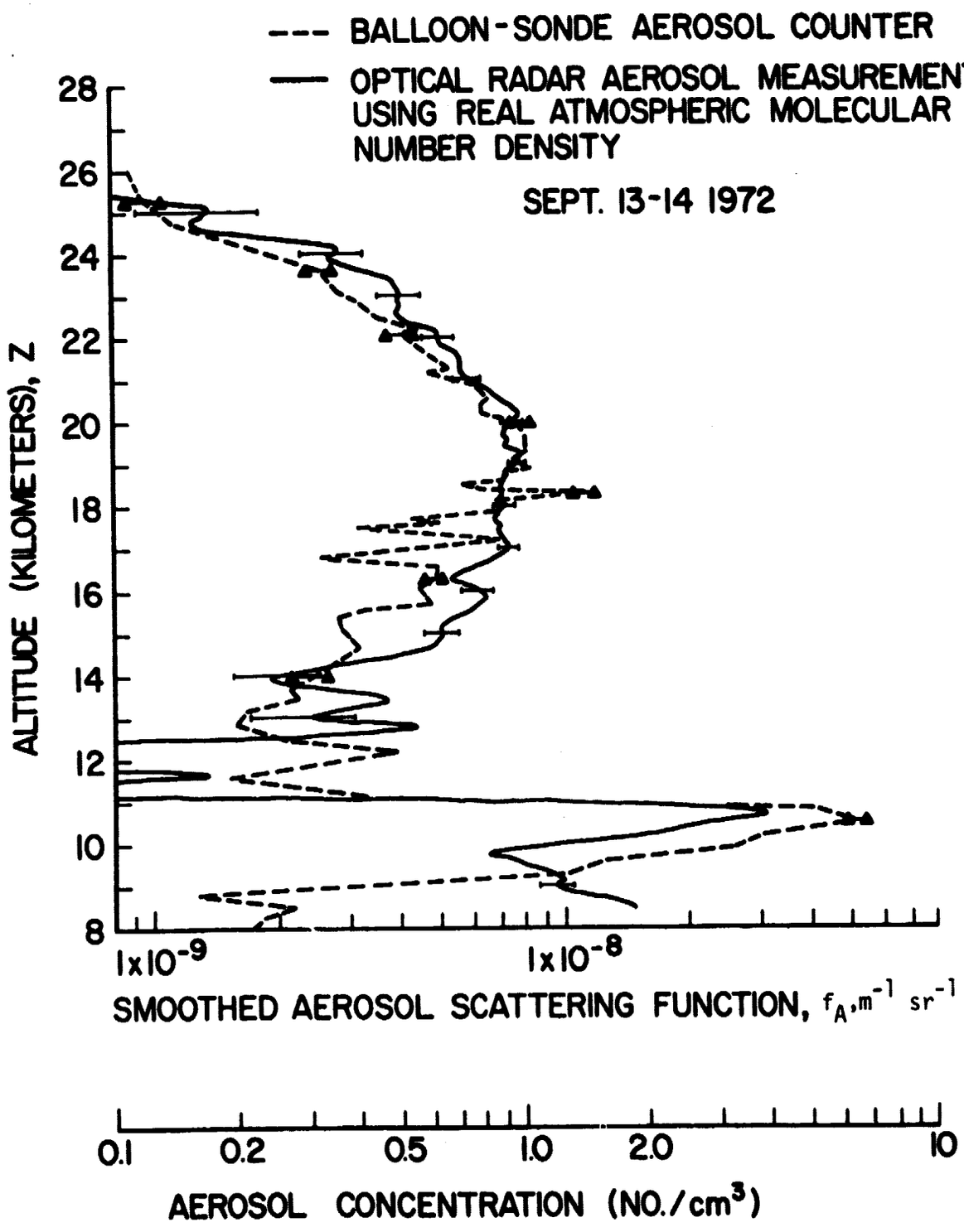

Figure 5.- Comparison of dustsonde particle concentration and lidar scattering function (9/13-14/72).

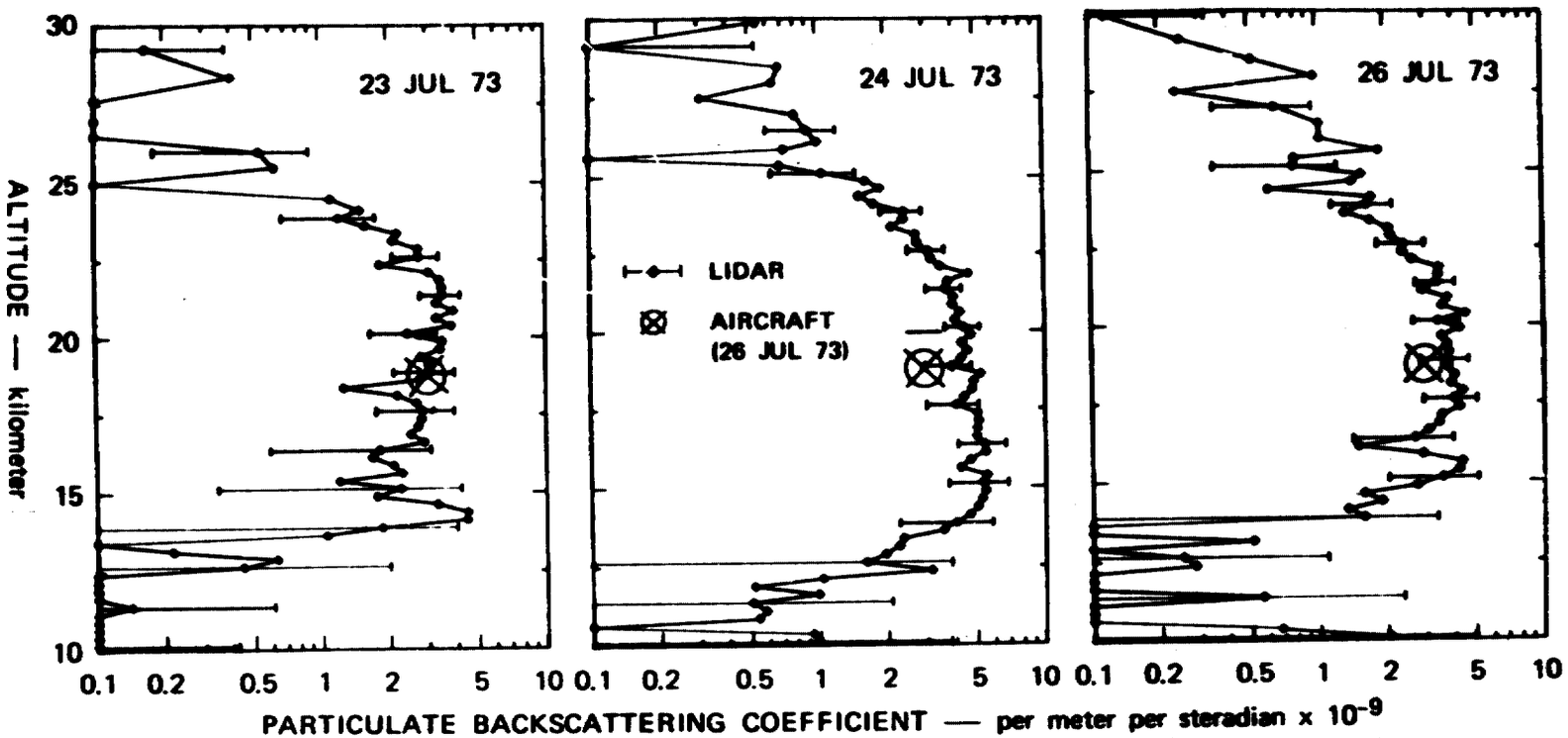

Figure 6.- Comparison of lidar backscatter with computed value based on aircraft mass-sampler measurement.

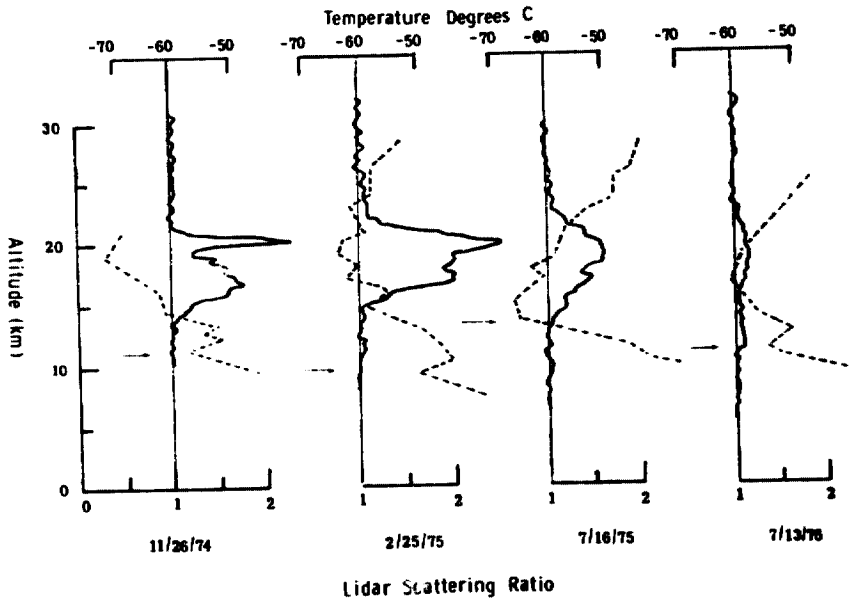

Figure 7.- Lidar backscatter profiles: Post-Fuego. The dashed lines are rawinsonde derived temperature profiles and the arrow indicates the location of the assumed tropopause.

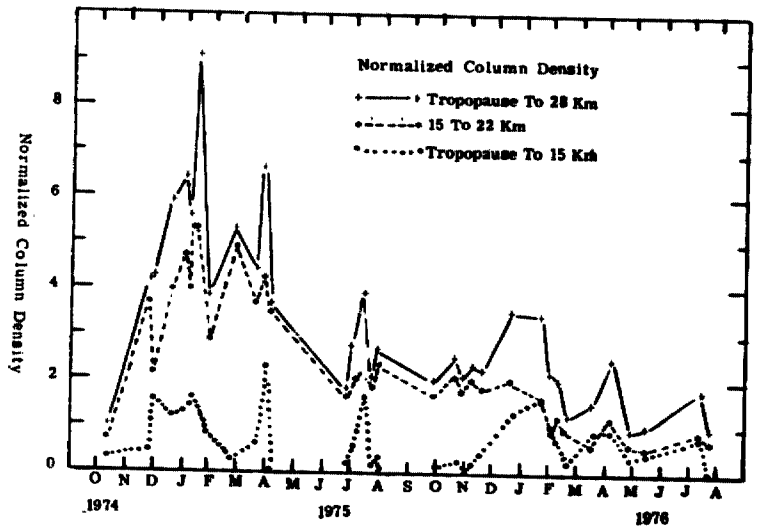

Figure 8.- Time variation of the normalized integrated backscatter for given stratospheric layers from October 1974 to July 1976.

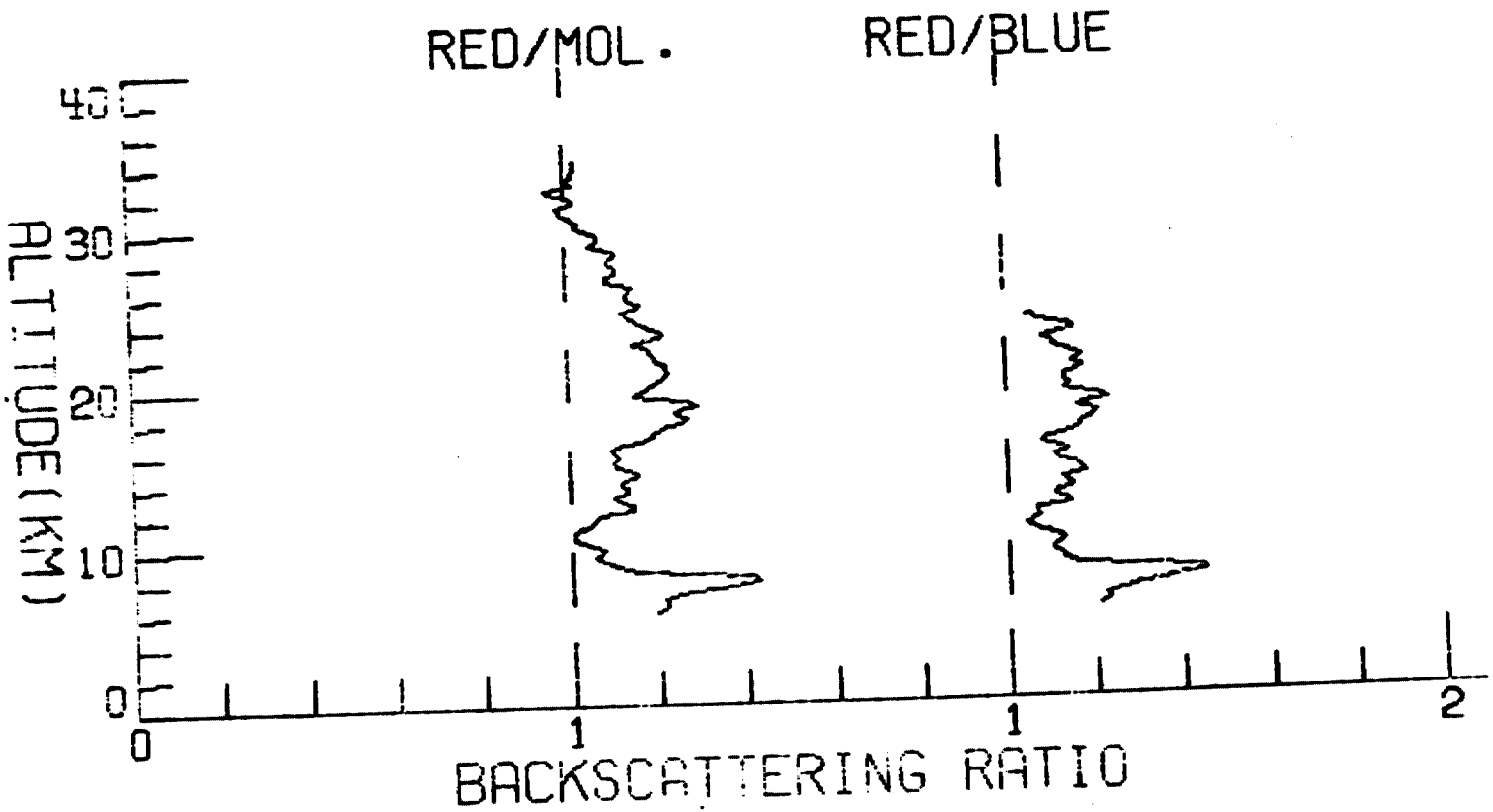

Figure 9.- Lidar backscatter ratios of RED/MOL and RED/BLUE for April 5, 1976.

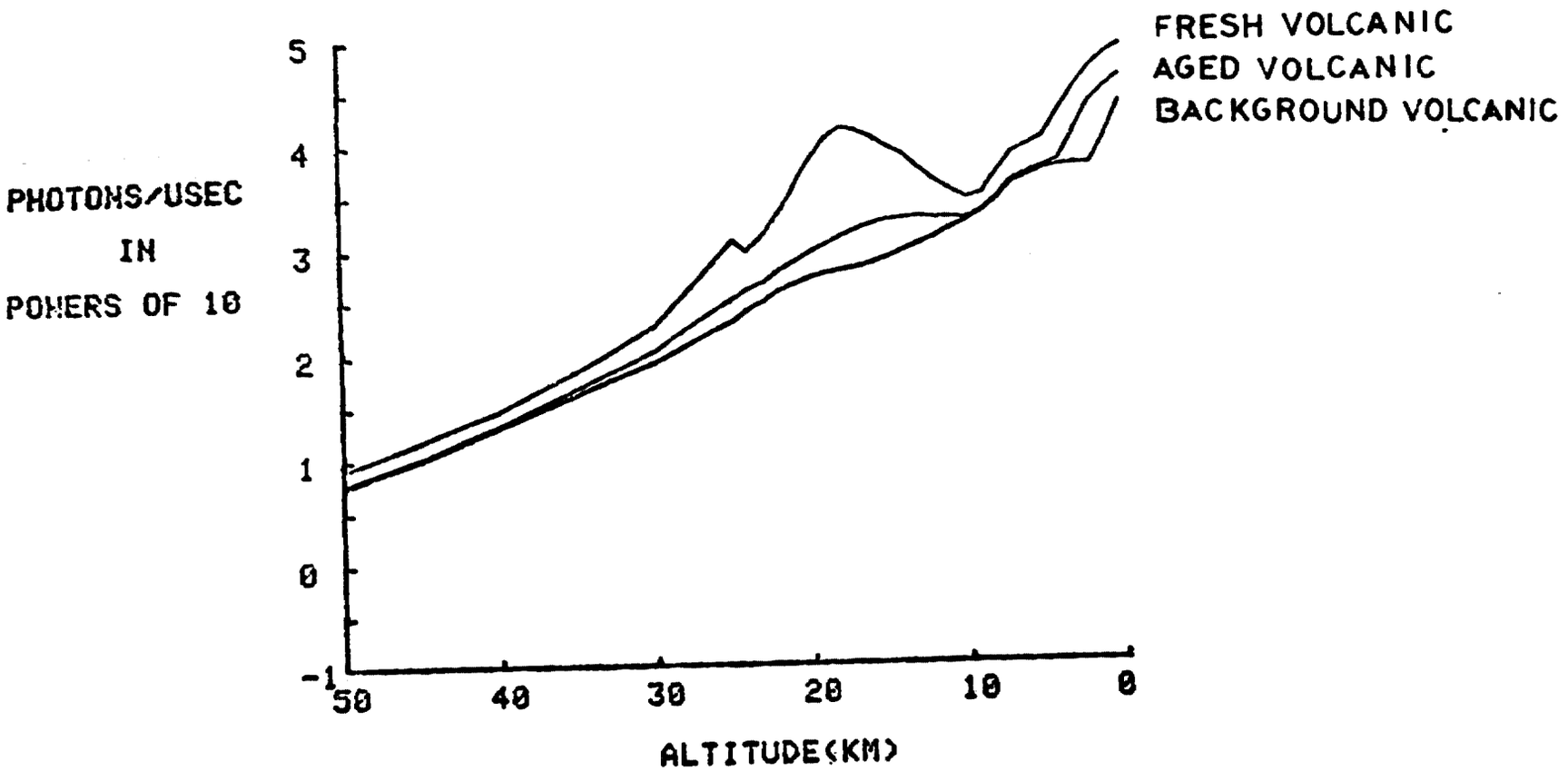

Figure 10.- Simulated lidar backscattered signal at a spacecraft altitude of 260 km incident on a 1-meter-diameter receiver. Simulation performed for various stratospheric aerosol models at scattering wavelength of 1.06 μm.

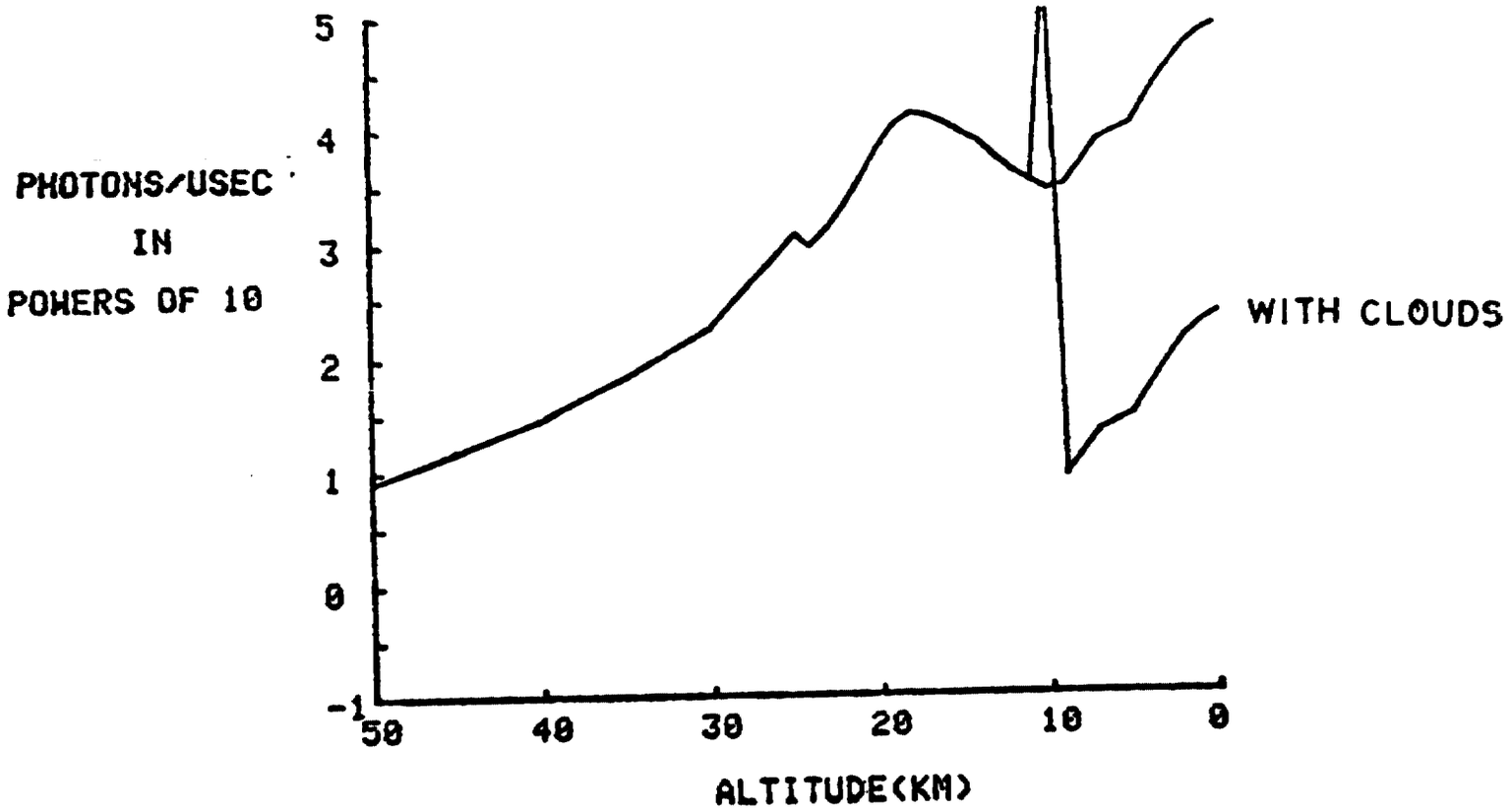

Figure 11.- Simulated lidar signal at 260 km with and without clouds at 10 km, for a 1-meter-diameter receiver and scattering wavelength of 1.06 μm assuming a fresh volcanic stratospheric aerosol model.

1. Report No.	2. Government Accession No.	3. Recipient's Catalog No.
NASA TM 74085		

4. Title and Subtitle	5. Report Date
The Use of Lidar for Stratospheric Measurements	September 1977
	6. Performing Organization Code 1250
7. Author(s)	8. Performing Organization Report No.
M. Patrick McCormick	
9. Performing Organization Name and Address	10. Work Unit No. 198-30-04-02
Langley Research Center Hampton, VA 23665	11. Contract or Grant No.
	13. Type of Report and Period Covered
12. Sponsoring Agency Name and Address	Technical Memorandum
National Aeronautics and Space Administration Washington, DC 20546	14. Sponsoring Agency Code
15. Supplementary Notes	

16. Abstract

This paper reviews stratospheric measurements possible with ground-based, airborne, and satellite-borne lidar systems. The instruments, basic equations, and formats normally used for various scattering and absorption phenomena measurements are presented including a discussion of elastic, resonance, Raman, and fluorescence scattering techniques.

17. Key Words (Suggested by Author(s))	18. Distribution Statement
Lidar (of laser radar), Atmospheric Scattering, Laser Applications, Stratosphere, Aerosols	Unclassified - Unlimited

19. Security Classif. (of this report)	20. Security Classif. (of this page)	21. No of Pages	22. Price*
Unclassified	Unclassified	24	$3.50

* For sale by the National Technical Information Service, Springfield Virginia 22161